Turkish Journal of Physics

http://journals.tubitak.gov.tr/physics/

Research Article

Turk J Phys
(2020) 44: 450 – 457

doi:10.3906/fiz-2004-17

Stable anisotropic single-layer of $ReTe_2$: a first principles prediction

Mehmet YAĞMURCUKARDEŞ*
Department of Physics, Faculty of Science, University of Antwerp, Antwerp, Belgium

Received: 20.04.2020 • **Accepted/Published Online:** 17.09.2020 • **Final Version:** 30.10.2020

Abstract: In order to investigate the structural, vibrational, electronic, and mechanical features of single-layer $ReTe_2$ first-principles calculations are performed. Dynamical stability analyses reveal that single-layer $ReTe_2$ crystallize in a distorted phase while its 1H and 1T phases are dynamically unstable. Raman spectrum calculations show that single-layer distorted phase of $ReTe_2$ exhibits 18 Raman peaks similar to those of ReS_2 and $ReSe_2$. Electronically, single-layer $ReTe_2$ is shown to be an indirect gap semiconductor with a suitable band gap for optoelectronic applications. In addition, it is found that the formation of Re-units in the crystal induces anisotropic mechanical parameters. The in-plane stiffness and Poisson ratio are shown to be significantly dependent on the lattice orientation. Our findings indicate that single-layer form of $ReTe_2$ can only crystallize in a dynamically stable distorted phase formed by the Re-units. Single-layer of distorted $ReTe_2$ can be a potential in-plane anisotropic material for various nanotechnology applications.

Key words: Density functional theory, in-plane anisotropic 2D materials, phonons and vibrational spectrum

1. Introduction

Successful exfoliation of graphene[1] from its layered bulk from, namely graphite, has rapidly grown interest in ultrathin two dimensional (2D) materials over last two decades. A particular attention among the 2D materials has been put on transition metal dichalcogenides (TMDs) which hold potential in optoelectronic device applications owing to their varying electronic properties[2–5].

Following the 2D forms of in-plane isotropic materials, 2D ultrathin crystals exhibiting in-plane anisotropy have been successfully saved into 2D library. The first 2D in-plane anisotropic single-layer has been demonstrated in 2014, black phosphorus (BP), which has been reported to exhibit polarization-dependent optical and vibrational properties and also in-plane anisotropic electronic, thermal, and mechanical features.[6–11] Apart from single-layer BP, many other anisotropic materials have been successfully synthesized such as semimetals (WTe_2, $MoTe_2$, $ZrTe_5$)[12–14] and semiconductors (group-IV monochalcogenides, GaTe, ReS_2, and $ReSe_2$)[15–18]. Among those semiconducting anisotropic materials, Re-dichalcogenides, with S and Se atoms, have been shown to possess layered bulk forms similar to other TMDs.[6, 7] The formation of diamond-like Re_4 clusters were shown to add unique anisotropic features to single-layers of Re-dichalcogenides.[19, 20] Zhong et al. investigated that the huge excitonic effects are dominant in the optical spectra of ReS_2 with an 1 eV of exciton binding energy.[21] On the other hand, it was shown that the ReS_2 layers are stacked and coupled in its few layer form confirmed by the Raman spectroscopy measurements.[22]

Searching for novel, stable, in-plane anisotropic single-layer materials is important in order to enlarge the family of those 2D structures. Motivated by the experimental realizations of Re-dichalcogenides, in this study,

*Correspondence: mehmetyagmurcukardes.edu@gmail.com

we predicted the possible structure of single-layer $ReTe_2$ which was shown to crystallize in distorted phase like ReS_2 and $ReSe_2$. The phonon band dispersions revealed that distorted phase of $ReTe_2$ is dynamically stable in contrast to its in-plane isotropic 1H and 1T phases. In addition, calculated Raman spectrum of $ReTe_2$ was shown to exhibit 18 Raman peaks that 7 of them are prominent. The electronic band dispersion calculations indicated that single-layer distorted $ReTe_2$ has a band gap of 0.83 eV. Moreover, the linear elastic mechanical constants, namely in-plane stiffness and Poisson ratio, were calculated using elastic stiffness tensor elements. Our results revealed the orientation-dependent behaviors of the elastic parameters that arise from the formed Re_4 units in the crystal structure.

2. Computational methodology

For the ab initio calculations, the plane wave basis projector augmented wave (PAW) method was considered with the generalized gradient approximation (GGA) of the Perdew–Burke–Ernzerhof (PBE) form which holds for the exchange and correlation potential[23] as implemented in the Vienna ab initio simulation package (VASP)[24]. The spin-orbit coupling (SOC) was taken into account for the electronic band calculations. The DFT-D2 method of Grimme was used to describe the van der Waals (vdW) interaction[25]. The charge transfers between the individual atoms was determined by the Bader technique.[26]

The kinetic energy cutoff was taken to be 500 eV while the energy difference between sequental steps was taken to be 10^{-8} eV. A width of 0.05 eV was used for Gaussian smearing while it was taken to be 0.1 for the phonon band dispersions. For the structural optimization a $24\times24\times1$ Γ-centered k-point samplings were used for the primitive unit cell, while for the density of states calculations it was doubled.

The phonon band structures were obtained by using the PHON code[27]. The corresponding Raman intensity of each vibrational mode was calculated such that the macroscopic dielectric tensor was differentiated with respect to each normal mode. For the calculation of the zone-centered phonon frequencies, the kinetic energy cutoff was increased to 800 eV.

The Raman activities are calculated within classical theory of polarizability based on Placzek's formula. In the theory, the Raman activity of a phonon mode is proportional to $|\hat{e}_s.R.\hat{e}_i|$ where $\hat{e}_s$ and $\hat{e}_i$ stand for the polarization vectors of the scattered radiation and incident light, respectively while R is the Raman tensor whose elements are the derivative of the polarizability with respect to each normal mode. Note that, for a phonon mode to be Raman active, R should include at least one nonzero element.

Table 1. For $ReTe_2$ phases; lattice parameters, a and b, bond distance corresponding to Re-Re and Re-Te bonds, d_{Re-Re} and d_{Re-Te}, respectively, the amount of charge donated to each Te atom by Re atom, $\triangle\rho$, and the electronic band gap, E_{gap}.

Structure	a (Å)	b (Å)	d_{Re-Re} (Å)	d_{Re-Te} (Å)	$\triangle\rho$ (e)	E_{gap} (eV)
1T$'$-$ReTe_2$	7.13	7.03	2.83-3.02	2.61-2.80	0.1	0.83

3. Results

3.1. Structural properties

In contrast to most of the TMDs, which crystallize either in 1T or 1H phases, single-layer of $ReTe_2$ is shown to possess its ground state in a distorted crystal form named as 1T-distorted (1T$'$) phase corresponding to

the point group symmetry C_i. In unitcell of 1T$^{'}$-$ReTe_2$, there are four Re atoms which form diamond-like Re_4 clusters while they are coordinated with eight Te atoms as shown in the Figure 1a. Although, 1H and 1T phases of single-layer $ReTe_2$ are shown to be energetically feasible, the 1T$^{'}$ phase is found to be the ground state structure for $ReTe_2$. As listed in Table 1, the lattice constants a and b are calculated as 7.13 and 7.03 Å, respectively with the angle between them to be 61.1 indicating the in-plane anisotropy. The atomic bond lengths between Re atoms forming the Re_4 clusters are found to be 2.83, 2.92, and 3.02 Å for different pairs, respectively. On the other hand, Re-Te bonds are formed with different bond distances due to the anisotropy in the crystall lattice. The Re-Te bond lengths are found to vary between 2.61 and 2.80 Å with all six bonds having different bond lengths. The Bader charge analysis reveal that while forming the single-layer 1T$^{'}$-$ReTe_2$, each Re atom donates its 0.1 e and totally 0.4 of e is donated to eight Te atoms indicating the covalent nature of the structure.

3.2. Dynamical stability and vibrational spectrum

The dynamical stability of single-layer phases of $ReTe_2$ were examined in terms of their phonon band dispersions. As shown in Figure 1b, the phonon branches are free from any imaginary frequencies for single-layer 1T$^{'}$-$ReTe_2$ while for 1H and 1T phases acoustic branches display imaginary behaviors through the Brillouin zone. As revelaed by the phonon band dispersions, only the 1T$^{'}$-$ReTe_2$ exhibits dynamical stability. Apart from three acoustic phonon branches, there are also thirty three optical branches with non-degeneracy due to anisotropy of the crystal.

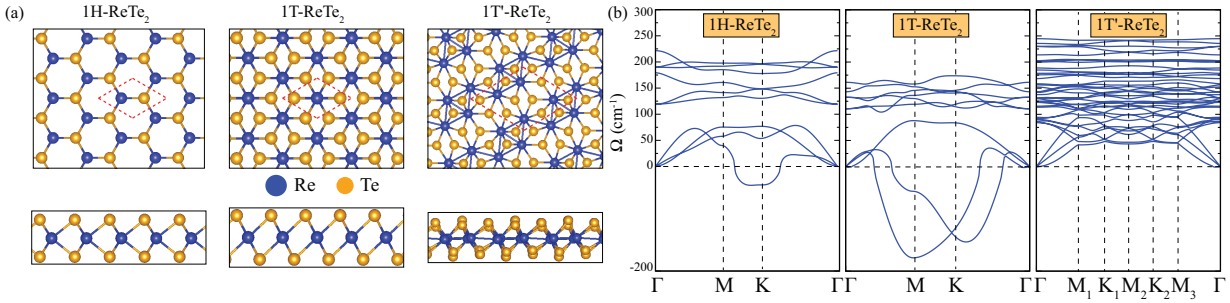

Figure 1. (a) Top and side views of 1H, 1T, and 1T$^{'}$ phases of single-layer $ReTe_2$. (b) The corresponding phonon band dispersions through the whole Brillouin zone.

Raman spectrum of single-layer 1T$^{'}$-$ReTe_2$ reveal that the eighteen modes are Raman active in which four phonon modes exhibit prominent Raman intensities indicating that they are observable in a Raman measurement. Those prominent Raman peaks are labeled as III, V, VI, and VII (see Figure 2a) while the other Raman active modes are found to possess very small intensities. The zone-centered frequencies of those prominent peaks are calculated to be 138, 215, 230, and 237 cm^{-1}, respectively. For the most prominent seven Raman active modes (labeled from I-to-VII), the vibrational motions of the atoms are given in Figure 2b. The two of the Raman active modes, namely I and II, arise from the pure in-plane vibration of the Re and Te atoms while the other five modes have both in-plane and out-of-plane motions. Apparently, in all seven Raman active modes, both Re and Te atoms contribute to the vibrations. Note that, the anisotropic nature of the single-layer 1T$^{'}$-$ReTe_2$ provides a rich Raman spectrum with its totally 18 Raman active phonon modes.

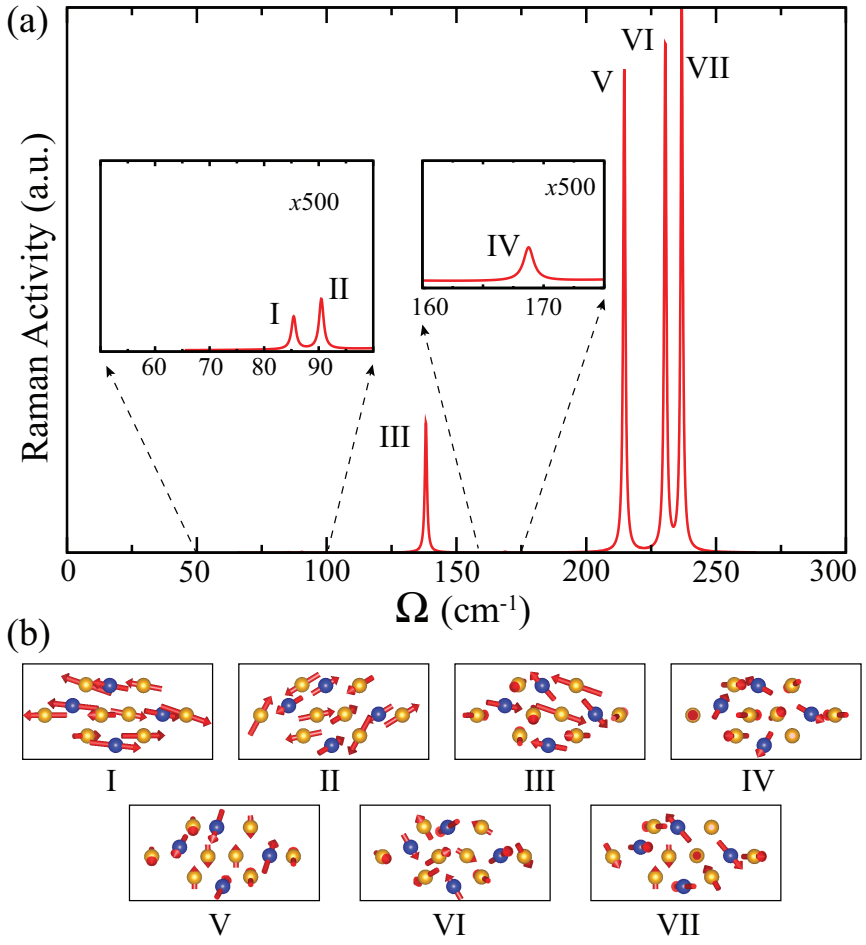

Figure 2. (a) Raman spectrum of single-layer 1T′-$ReTe_2$. Inset shows the two weak-intensity peaks. (b) The atomic vibrations in seven prominent Raman active phonon modes.

3.3. Electronic properties

As shown in Figure 3, single-layer 1T′-$ReTe_2$ has a band gap of 0.83 eV calculated within GGA+SOC. The valence band (VB) and the conduction band (CB) edges reside at K_2/Γ and Γ/K_1, respectively. The predicted band gap of single-layer 1T′-$ReTe_2$ (see Table 1) is much smaller than that of single-layer ReS_2 (1.34 eV)[20]. The spin-orbit splitting is calculated to be 10 meV at the Γ point. The band gap of single-layer 1T′-$ReTe_2$ is comparable to that of well-known anisotropic single-layer blackphosphorus (0.57 eV)[6]. The atomic orbital contributions to the VB and CB edges are analyzed by calculating the corresponding partial density of states. Partial density of states analysis reveals that Re-d and Te-p orbitals hybridize in order to form Re-Te bonds contributing to the VB edges. In addition, the CB edge is dominated by the unoccupied Re-d orbitals while the Te-p orbitals have smaller contribution.

3.4. Anisotropic mechanical properties

The in-plane stiffness, C, and the Poisson ratio, ν, are two independent elastic parameters indicating the linear elastic behaviors. In order to obtain those two parameters, the elastic stiffness tensor is calculated and

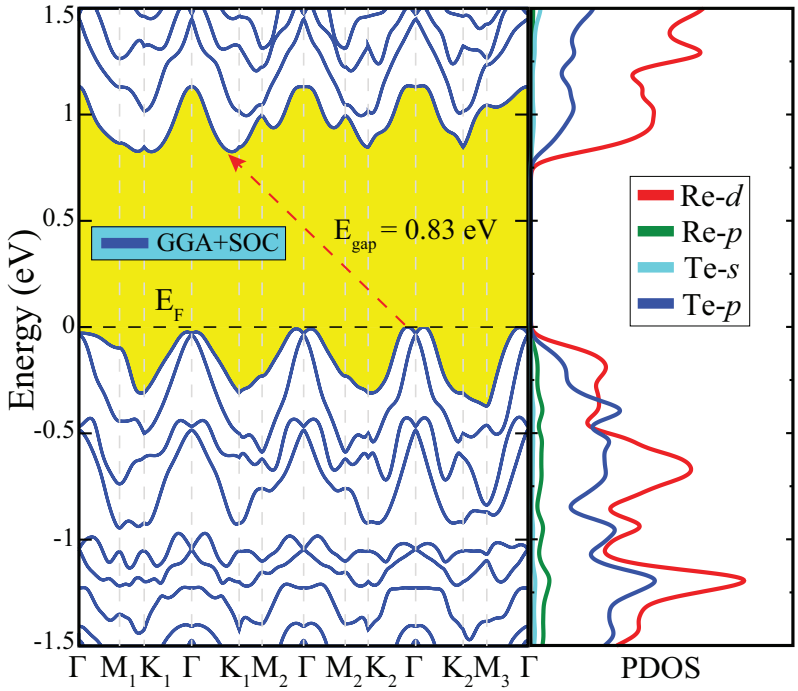

Figure 3. Electronic band structure (on the left) with partial density of states (on the right) for single-layer 1T′-$ReTe_2$. The Fermi energy is set to zero level.

the corresponding tensor elements, C_{ij}, are obtained. Once the C_{ij} are calculated, the orientation angular dependency of the C and ν are calculated using the formulas given below:

$$C(\theta) = \frac{(C_{11}C_{22} - C_{12}^2)}{C_{22}cos^4(\theta) + Acos^2(\theta)sin^2(\theta) + C_{11}sin^4(\theta)}, \tag{1}$$

and

$$\nu(\theta) = \frac{C_{12}cos^4(\theta) - Bcos^2(\theta)sin^2(\theta) + C_{12}sin^4(\theta)}{C_{22}cos^4(\theta) + Acos^2(\theta)sin^2(\theta) + C_{11}sin^4(\theta)}. \tag{2}$$

Here, the numbers A and B are defined such that A=($C_{11}C_{22}$-$C_{12}C_{21}$)/C_{66}-2C_{21} and B=C_{11}+C_{22}-($C_{11}C_{22}$-$C_{12}C_{21}$)/C_{66}. C is known as the measure of flexibility of a material in the linear elastic regime. Graphene has the highest stiffness (330 N/m)[28] among the 2D materials. As a promising in-plane anisotropic single-layer, ReS_2 exhibits 166 and 159 N/m of stiffness values for two main orientation[28]. Our results reveal that single-layer 1T′-$ReTe_2$ possesses 94 and 105 N/m stiffness along the directions perpendicular and parallel to the Re_4 units, respectively. Apparently, the formation of Re_4 units makes the material quite stiffer along a certain direction. As shown in Figure 4a, the orientation dependency of the in-plane stiffness does not display strong in-plane anisotropy.

On the other hand, ν is defined as the ratio of longitudinal extension to the transverse contraction. As mentioned above, the Poisson ratio and the in-plane stiffness are two independent constants. The Poisson ratio is calculated to be 0.23 and 0.25 along the directions perpendicular and parallel to the Re_4 units, respectively.

Notably, these two values are larger than those of ReS_2 (0.19 for both orientations) while they are close to that of single-layer MoS_2 (0.26).[28] The values reveal quite strong ability of single-layer 1T′-$ReTe_2$ for preserving its equilibrium structural state when subjected to external applied loads.

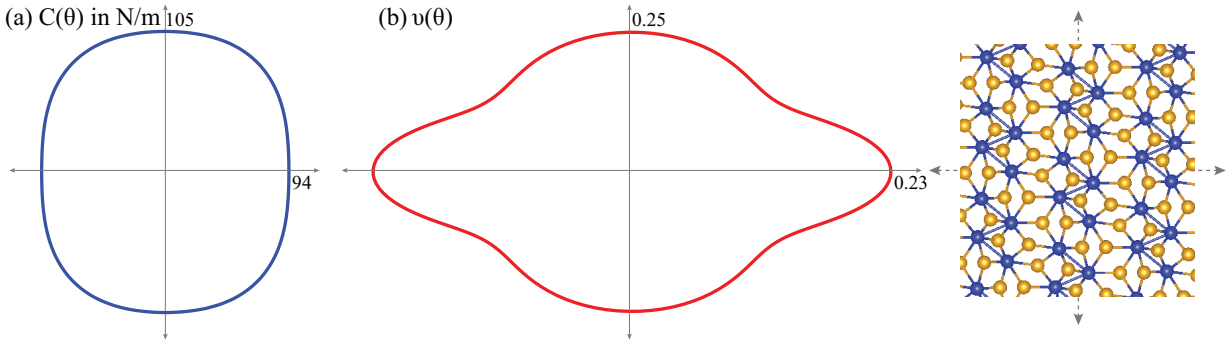

Figure 4. For the in-plane anisotropic single-layer 1T′-$ReTe_2$ angle-dependent; (a) in-plane stiffness and (b) the Poisson ratio. On the right the top view of the structure is given to identicate the orientation directions.

4. Conclusion

In the present work, we proposed the dynamically stable single-layer phase of $ReTe_2$, in-plane anisotropic 2D material. The structural, electronic, vibrational, and mechanical properties of single-layer 1T′-$ReTe_2$ were investigated. Dynamical stability analyses revealed that single-layer $ReTe_2$ crystallize in a distorted phase, namely 1T′-$ReTe_2$, while its 1H and 1T phases were shown to be dynamically unstable. Raman spectrum calculations showed that single-layer distorted phase of $ReTe_2$ exhibits 18 Raman peaks only 4 of them were revealed to be prominent. Electronically, single-layer $ReTe_2$ was shown to be a semiconductor with a suitable band gap for optoelectronic applications. In addition, the formation of Re_4-units in the crystal were shown to create in-plane anisotropy in elastic constants. The calculated in-plane stiffness and the Poisson ratio were shown to be dependent on the lattice orientation. Our findings revealed that single-layer form of $ReTe_2$ can only crystallize in a dynamically stable distorted phase formed by the diamond-like Re_4-units. Single-layer of distorted $ReTe_2$ can be a potential in-plane anisotropic material for various nanotechnology applications.

Acknowledgment

Computational resources were provided by the Scientific and Technological Research Council of Turkey (TÜBİTAK) Turkish Academic Network and Information Center (ULAKBİM), High Performance and Grid Computing Center (TR-Grid e-Infrastructure) and by Flemish Supercomputer Center (VSC). This work was supported by the Flemish Science Foundation (FWO-Vl) by a postdoctoral fellowship (M.Y.).

References

[1] Novoselov KS, Geim AK, Morozov SV, Jiang D, Zhang Y et al. Electric field effect in atomically thin carbon films. Science 2004; 306 (5696): 666-669. doi: 10.1126/science.1102896

[2] Neto AHC, Novoselov KS. New directions in science and technology: two-dimensional crystals. Reports on Progress in Physics 2011; 74 (8): 082501. doi: 10.1088/0034-4885/74/8/082501

[3] Kasowski RV. Band Structure of MoS_2 and NbS_2. Physical Review Letters 1973; 30: 1175. doi: 10.1103/PhysRevLett.30.1175

[4] Ye JT, Zhang JY, Akashi R, Bahramy MS, Arita R et al. Superconducting dome in a gate-tuned band insulator. Science 2012; 338: 1193. doi: 10.1126/science.1228006

[5] Splendiani A, Sun L, Zhang Y, Li T, Kim J et al. Emerging photoluminescence in monolayer MoS_2. Nano Letters 2010; 10: 1271. doi: 10.1021/nl903868w

[6] Li L, Yu Y, Ye GJ, Ge Q, Ou X et al. Black phosphorus field-effect transistors. Nature Nanotechnology 2014; 9 (5): 372-377. doi: 10.1038/nnano.2014.35

[7] Xia F, Wang H, Jia Y. Rediscovering black phosphorus as an anisotropic layered material for optoelectronics and electronics. Nature Communications 2014; 5: 4458. doi: 10.1038/ncomms5458

[8] Jiang H, Shi H, Sun X, Gao B. Optical anisotropy of few-layer black phosphorus visualized by scanning polarization modulation microscopy. ACS Photonics 2018; 5 (6): 2509-2515. doi: 10.1021/acsphotonics.8b00341

[9] Zhang G, Huang S, Chaves A, Song C, Özçelik VO et al. Infrared fingerprints of few-layer black phosphorus. Nature Communications 2017; 8: 14071. doi: 10.1038/ncomms14071

[10] Wu J, Mao N, Xie L, Xu H, Zhang J. Identifying the crystalline orientation of black phosphorus using angle-resolved polarized raman spectroscopy. Angewandte Chemie International Edition 2015; 127 (8): 2396- 2399. doi: 10.1002/anie.201410108

[11] Qiao J, Kong X, Hu Z-X, Yang F, Ji W. High-mobility transport anisotropy and linear dichroism in few-layer black phosphorus. Nature Communications 2014; 5: 4475. doi: 10.1038/ncomms5475

[12] Torun E, Sahin H, Cahangirov S, Rubio A, Peeters FM. Anisotropic electronic, mechanical, and optical properties of monolayer WTe_2. Journal of Applied Physics 2016; 119: 074307. doi: 10.1063/1.4942162

[13] Song S, Keum DH, Cho S, Perello D, Kim Y et al. Room temperature semiconductor-metal transition of $MoTe_2$ thin films engineered by strain. Nano Letters 2015; 16 (1): 188-193. doi: 10.1021/acs.nanolett.5b03481

[14] Weng H, Dai X, Fang Z. Transition-metal pentatelluride $ZrTe_5$ and $HfTe_5$: a paradigm for large-gap quantum spin hall insulators. Physical Review X 2014; 4: 011002. doi: 10.1103/PhysRevX.4.011002

[15] Huang S, Tatsumi Y, Ling X, Guo H, Wang Z et al. In-plane optical anisotropy of layered gallium telluride. ACS Nano 2016; 10 (9): 8964-8972. doi: 10.1021/acsnano.6b05002

[16] Fei R, Li W, Li J, Yang L. Giant piezoelectricity of monolayer group IV monochalcogenides: SnSe, SnS, GeSe, and GeS. Applied Physics Letters 2015; 107 (17): 173104. doi: 10.1063/1.4934750

[17] Wolverson D, Crampin S, Kazemi AS, Ilie A, Bending SJ. Raman spectra of monolayer, few-layer, and bulk $ReSe_2$: an anisotropic layered semiconductor. ACS Nano 2014; 8 (11): 11154-11164. doi: 10.1021/nn5053926

[18] Tongay S, Sahin H, Ko C, Luce A, Fan W et al. Monolayer behaviour in bulk ReS_2 due to electronic and vibrational decoupling. Nature Communications 2015; 5: 3252. doi: 10.1038/ncomms4252

[19] Hafeez M, Gan L, Li H, Ma Y, Zhai T. Large-area bilayer ReS_2 film/multilayer ReS_2 flakes synthesized by chemical vapor depo- sition for high performance photodetectors. Advanced Functional Materials 2016; 26 (26): 4551-4560. doi: 10.1002/adfm.201601019

[20] Yagmurcukardes M, Bacaksiz C, Senger RT, Sahin H. Hydrogen-induced structural transition in single layer ReS_2. 2D Materials 2017; 4 (3): 035013. doi: 10.1088/2053-1583/aa78c8

[21] Zhong HX, Gao S, Shi JJ, Yang L. Quasiparticle band gaps, excitonic effects, and anisotropic optical properties of the monolayer distorted 1T-diamond-unit structures ReS_2 and $ReSe_2$. Physical Review B 2015; 92: 115438. doi: 10.1103/PhysRevB.92.115438

[22] Chenet DA, Aslan OB, Huang PY, Fan C, Van der Zande AM et al. In-plane anisotropy in mono- and few-layer ReS_2 probed by Raman spectroscopy and scanning transmission electron microscopy. Nano Letters 2015; 15 (9): 5667-5672. doi: 10.1021/acs.nanolett.5b00910

[23] Perdew JP, Burke K, Ernzerhof M. Generalized gradient approximation made simple. Physical Review Letters 1996; 77: 3865. doi: 10.1103/PhysRevLett.77.3865

[24] Kresse G, Hafner J. Ab initio molecular dynamics for liquid metals. Physical Review B 1993; 47: 558. doi: 10.1103/PhysRevB.47.558

[25] Grimme SJ. Semiempirical GGA-type density functional constructed with a long-range dispersion correction. Journal of Computational Chemistry 2006; 27 (26): 1787. doi: 10.1002/jcc.20495

[26] Henkelman G, Arnaldsson A, Jonsson H. A fast and robust algorithm for Bader decomposition of charge density. Computational Material Science 2006; 36: 354. doi: 10.1016/j.commatsci.2005.04.010

[27] Alfe D. PHON: a program to calculate phonons using the small displacement method. Computer Physics Communications 2009; 180: 2622. doi: 10.1016/j.cpc.2009.03.010

[28] Yagmurcukardes M, Bacaksiz C, Unsal E, Akbali B, Senger RT et al. Strain mapping in single-layer two-dimensional crystals via Raman activity. Physical Review B 2018; 97: 115247. doi: 10.1103/PhysRevB.97.115427